Simple constitutive models to study the influence of installation damage on the load-strain response of two geogrids

António M. Paula
Polytechnic Institute of Bragança, Portugal

Margarida Pinho-Lopes
University of Southampton, United Kingdom

ABSTRACT: A key factor affecting the tensile response of geosynthetics is installation damage, represented by a reduction factor capturing changes in tensile strength. Although often geosynthetics are represented in numerical models by simple linear-elastic constitutive models and a stiffness, the response of geosynthetics to loading can be represented more realistically by non-linear constitutive models. Herein, simple constitutive models were used to represent the short-term tensile response of two geogrids (woven geogrid and uniaxial extruded geogrid). The tensile response of samples exhumed after field installation under real conditions was compared to that of the corresponding undamaged samples (as-received). The changes in response, particularly the change in tensile strength and stiffness, were presented and discussed. The polynomial models (order 6) approximated the experimental data better than the hyperbolic models. Contrary to what has been reported in the literature, for the materials and test conditions presented herein and for the hyperbolic models, the parameter b cannot be estimated as the inverse of the materials tensile strength and the parameter α is not a material constant. Both polynomial and hyperbolic models approximated well the tangent stiffness for 2% strain obtained experimentally. The model parameters were normalised to the reduction factor for installation damage; for the hyperbolic models, the parameter b was practically unchanged after exhumation of the samples, while parameters a and α showed no clear trend; the values of the stiffness normalised to the reduction factor for installation damage were not constant.

Keywords: constitutive models, geogrids, installation damage, tensile response, stiffness, reduction factor

1 INTRODUCTION

The design of geosynthetics often relies on the definition of their tensile properties. Particularly for soil reinforcement applications, the relevant design parameters are usually the tensile strength and strain. Numerical models, namely using the finite element method (FEM), are becoming more and more popular to assist the design of reinforced soil structures and/or analyse their performance. Often, in such models, geosynthetics are represented by simple linear-elastic constitutive models, i.e., a stiffness (sometimes a tensile strength can be included). However, the response of geosynthetics to loading can be represented more realistically by non-linear constitutive models. In the literature, there are proposals for simple constitutive models to represent the stress-strain response of geosynthetics. In most cases, such models reproduce the short-term or the long-term tensile response of geosynthetics, for materials tested as-received and in-isolation.

The tensile properties of geosynthetics may be significantly impacted by installation damage, which may reduce the available tensile strength, strain and stiffness. In most codes / guides, the effect of installation damage on the tensile strength of geosynthetics is represented by a reduction factor. Usually this factor is defined as the ratio of the initial tensile strength (for an undamaged sample) to that after installation damage under real project conditions (soil, compaction conditions) or similar. However, using this reduction factor only captures changes in ultimate tensile strength. Installation damage may also reduce the stiffness of geosynthetics, with smaller reductions than for the tensile strength. In particular, for wo-

ven materials and uniaxial geogrid products, the stiffness can quantify the resistance to installation damage under real conditions better than the tensile strength (Allen and Bathurst 1994, Pinho-Lopes and Lopes 2014).

To define relevant values of properties of geosynthetics (tensile strength and stiffness) to be used in numerical analysis, in this paper the short-term tensile response of two geogrids was analysed and approximated using simple constitutive models. The geosynthetics were exhumed after installation damage under real conditions and the changes in the constitutive models and the corresponding parameters were analysed.

2 SIMPLE CONSTITUTIVE MODELS

Herein two types of simple constitutive models were used to represent the short-term load-strain response of geosynthetics: polynomial models and hyperbolic models.

The short-term response of geosynthetics has been represented using polynomial models (Equation 1),

$$T = \sum_{i=0}^{n} a_i \varepsilon^i \tag{1}$$

where T is the load per unit width, ε is the axial tensile strain in the geosynthetic, a_i is the polynomial coefficient of order i and n is the order of the polynomial.

Curve fitting of experimental data for particular geosynthetics, mostly using the least-squares method, is used to determine the polynomial coefficients (Bathurst and Kaliakin 2005). Using this approach, the stiffness of the geosynthetic can be estimated by differentiating Equation 1 with respect to strain (Equation 2). Such stiffness is the product between the instantaneous tangent modulus, E_t, and the initial cross-section, A, assumed constant, which is often used in numerical analysis.

$$AE_t = \frac{dT}{d\varepsilon} = \frac{d(\sigma A)}{d\varepsilon} = \sum_{i=1}^{n} a_i \varepsilon^{i-1} \tag{2}$$

The short-term response of geosynthetics can also be simulated using hyperbolic models, based on hyperbolic load-strain relationships (Bathurst and Kaliakin 2005). Depending on the type of tensile response observed (type A and B, Figure 2) two sets of models are used.

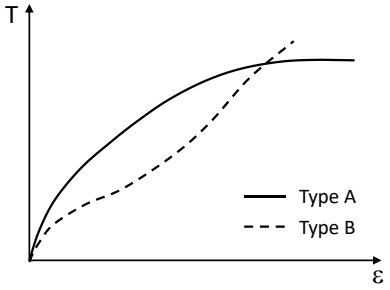

Figure 2. Typical load-strain relationships of geosynthetics - type A and type B (not to scale).

Liu and Ling (2006) proposed constitutive models to represent the cyclic tensile loading of geosynthetics, isolating the response for primary loading. Herein the equations proposed by these authors for primary loading behaviour are presented. For type A geosynthetics, the hyperbolic model suggested by Liu and Ling (2006), is represented by Equations 3 to 5, where *a* and *b* are constants (Equations 4 and 5, respectively), J_i is the initial stiffness and T_{ult} represents the ultimate strength of type A geosynthetics. Equation 6 represents the corresponding tangent stiffness for strain ε, $J_{t\,\varepsilon\%}$.

$$T = \frac{\varepsilon}{a + b\varepsilon} \tag{3}$$

$$a = \frac{1}{J_i} \tag{4}$$

$$b = \frac{1}{T_{ult}} \tag{5}$$

$$J_{t\,\varepsilon\%} = \frac{dT}{d\varepsilon} = \frac{a}{(a + b\varepsilon)^2} \tag{6}$$

For type B geosynthetics, Liu and Ling (2006) proposed using a nonlinear function combining a hyperbola (for low strains) with an exponential function (for high strains): Equation 7, where ε_{max} is the rupture

tensile strain of the geosynthetic, α is a material constant and 1/b is the tensile strength of the geosynthetic (Equation 5). The corresponding tangent stiffness, $J_{t\,\varepsilon\%}$, (type B materials) can be obtained from Equation 8.

$$T = \frac{\varepsilon}{a+2b\varepsilon} + \frac{1}{2b} \cdot e^{-\alpha(\varepsilon-\varepsilon_{max})^2} \quad (7)$$

$$J_{t\,\varepsilon\%} = \frac{dT}{d\varepsilon} = \frac{a}{a+2b\varepsilon} + \frac{-\alpha(\varepsilon-\varepsilon_{max})}{b} \cdot e^{-\alpha(\varepsilon-\varepsilon_{max})^2} \quad (8)$$

Hyperbolic-based models are very simple to implement and make use of a small number of parameters, which can be calibrated for specific geosynthetics using tests results (Bathurst and Kaliakin 2005).

3 MATERIALS AND FIELD INSTALLATION TESTS

This paper includes results for two geogrids (Figure 1): a woven geogrid (GGRw), formed by high tenacity polyester (PET) yarns woven into a grid structure and covered with black polymeric coating; and a high density polyethylene (HDPE) uniaxial extruded geogrid (GGRu).

a) b)

Figure 1. Geosynthetics studied: a) GGRw; b) GGRu.

The load-strain response of the geogrids was measured using wide-width tensile tests (BSI 2008, EN ISO 10319), for both undamaged specimens and specimens exhumed after installation. For each sample, five specimens were tested using hydraulic jaws; the strains were measured using a video-extensometer; all specimens were tested in the machine direction.

Trial embankments were built, where the geosynthetics were installed between layers of compacted material. Each embankment was formed by a foundation layer (built over a road base) where the geosynthetics were placed, and two layers of compacted soil. All these three layers were formed by the same soil and were 0.20m high each, after compaction. The soil was a well-graded gravel with silt (soil S3 in Pinho-Lopes and Lopes 2014; D_{50}=9.88mm; D_{max}=50mm). Two different compaction energies were used, defined as a fraction of the normal Proctor of the soil (90%, CE1 and 98%, CE2). After completion, the embankments were dismantled and the geosynthetics were recovered for testing.

4 RESULTS AND DISCUSSION

Results from experimental data were approximated using simple constitutive models, polynomial and hyperbolic-based models (described in section 2). To ensure the models replicated the response of the geogrids realistically, the data used for the fitting exercise excluded data points after the failure of the specimens.

4.1 *Base experimental data*

Table 1 summarises the tensile tests results and includes: tensile strength, T_{max}; strain for maximum load, ε_{max}; secant stiffness for 2% strain, $J_{s\,2\%}$, (Equation 9, where $T_{2\%}$ is the force for 2% strain). The results refer to five valid specimens per sample and include the corresponding coefficient of variation (CV).

$$J_{s\,2\%} = \frac{T_{2\%} \times 100}{2} \quad (9)$$

Figure 3 illustrates some of the load-strain responses obtained experimentally; for clarity, the figure includes data for one representative specimen per sample. Two different types of responses were observed: type A, for GGRu, and type B for GGRw.

Table 1. Summary of the tensile tests results for GGRw and GGRu for different types of samples: undamaged (UND) and exhumed after installation damage with compaction energy CE1 and CE2 (ID CE1 and ID CE2, respectively)

Property		GGRw			GGRu		
		UND	ID CE1	ID CE2	UND	ID CE1	ID CE2
T_{max} (kN/m)	Mean	70.8	57.5	61.5	61.6	57.7	50.6
	CV (%)	4.3	7.9	7.5	5.0	3.1	11.1
ε_{max} (%)	Mean	16.0	15.2	14.9	17.1	14.5	11.4
	CV (%)	6.2	11.0	5.91	4.8	13.2	9.6
$J_{s\,2\%}$ (kN/m)	Mean	583.9	590.1	580.2	1024.3	980.4	931.4
	CV (%)	1.0	1.0	1.1	6.7	6.3	1.4

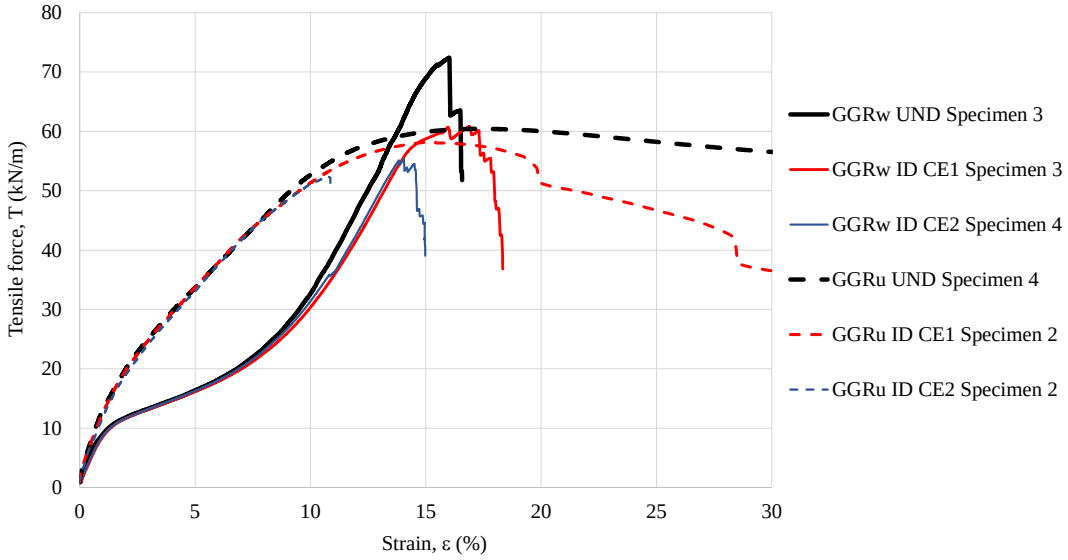

Figure 3. Tensile response of the GGRw and GGRu, undamaged (UND) and exhumed after installation damage (ID CE1 and IDC E2).

4.2 *Simple models*

The experimental data was fitted with two simple models. For each sample, undamaged (UND) and exhumed after installation damage (ID CE1 and ID CE2), one polynomial model of order 6 (Equation 1, with n=6) and a hyperbolic-based model (Equation 3 for GGRu or Equation 7 for GGRw) were used to fit the data for each specimen tested. Then the average value of each parameter (for five specimens per sample) was determined. For the polynomial models all parameters a_i (from Equation 1) were obtained from the curve fitting exercise. For the hyperbolic-based models two approaches were used: 1) the parameter b was fixed for each specimen (using Equation 5) and the other parameters (a, and α when applicable) were optimised from the curve fitting exercise; 2) all parameters (a, b, and α when applicable) were obtained by curve fitting. The results are summarised in Table 2, where the average values obtained for model parameters and the coefficient of determination (R^2) are shown, and in Figure 4, which summarises the models used to fit the tensile experimental data for the two geogrids for selected specimens.

For both geogrids, the polynomial models fit the experimental data very well (R^2~1.0 and CV between 0.01% and 0.09%); however, these are simple mathematical functions fitted to the data, with no physical meaning. The hyperbolic-based models defined for a fixed value of b (as a function of the tensile strength of each specimen) do not match the experimental data well, as they cannot capture the shape of the load-strain curves of the specimens, for both GGRw and GGRu (Figure 4). Thus, hyperbolic-based models where all parameters were obtained from curve fitting the experimental data were determined. In these cases, although the hyperbolic-based models with all parameters varying fit well the experimental data, they are not able to replicate the response observed for the full range of strains measured, particularly for GGRw (Figure 4a), as they do not capture the full change in curvature of the load-strain curves. The values of the parameter b are plotted against the inverse of the each specimen's tensile strength in Figure 5, for the models with all parameters optimised during curve fitting. This confirms that Equation 5 does not represent the relationship between the two quantities for the data included herein, particularly for GGRu.

Table 2. Parameters obtained for the simple constitutive models for GGRw and GGRu for different types of samples: undamaged (UND) and exhumed after installation damage with compaction energy CE1 and CE2 (ID CE1 and ID CE2, respectively) – average of parameters obtained for five specimens per sample and coefficient of variation (CV) for some parameters.

Model	Parameter	GGRw			GGRu		
		UND	ID CE1	ID CE2	UND	ID CE1	ID CE2
Polynomial (n=6)	a_0	1.6208	1.0440	0.9579	1.4537	1.7713	1.0157
	a_1	9.1980	10.8300	10.5200	14.1000	12.9240	12.3040
	a_2	-2.9414	-4.0970	-3.7660	-3.1496	-2.8364	-2.2144
	a_3	0.5302	0.8591	0.7421	0.5119	0.4939	0.2390
	a_4	-0.0508	-0.0950	-0.0766	-0.0437	-0.0483	-0.0005
	a_5	0.0027	0.0055	0.0042	0.0018	0.0024	-0.0018
	a_6	-0.0001	-0.0001	-0.0001	0.0000	-0.0001	0.0001
	R^2	0.9997	0.9999	1.0000	0.9999	0.99976	0.99958
	CV for R^2	0.01%	0.04%	0.02%	0.01%	0.04%	0.09%
Hyperbolic-based ($b=1/T_{ult}$)	a	0.1125	0.1025	0.1151	0.0479	0.0497	0.0483
	CV for a	4.80%	4.90%	7.40%	7.20%	5.90%	10.20%
	b	0.0141	0.0175	0.0163	0.0163	0.0173	0.0200
	CV for b	4.50%	8.10%	7.60%	4.60%	3.20%	12.40%
	α	0.0449	0.0505	0.0595	-	-	-
	CV for α	40%	55%	23%	-	-	-
	R^2	0.9767	0.9828	0.9902	0.9067	0.9093	0.9053
	CV for R^2	1.20%	1.20%	0.30%	0.29%	0.46%	0.42%
Hyperbolic-based	a	0.1704	0.1317	0.1360	0.0838	0.0882	0.0886
	CV for a	11.6%	19.70%	13.00%	7.2%	8.20%	11.70%
	b	0.0122	0.0159	0.0152	0.0107	0.0110	0.0122
	CV for b	9.10%	14.50%	10.10%	4.60%	4.90%	22.20%
	α	0.0512	0.0562	0.0667	-	-	-
	CV for α	37%	48%	21%	-	-	-
	R2	0.9958	0.9941	0.9951	0.9940	0.9948	0.9937
	CV for R2	0.20%	0.20%	0.10%	0.01%	0.60%	0.30%

The data in Table 2 also indicates that for GGRw the parameter α is not a material constant, contrary to what was reported by Liu and Ling (2006), as it varies significantly for each sample. For example, for the undamaged sample, for the hyperbolic-based model with b fixed the average value of α is 0.0449 and CV=40% and for the hyperbolic-based model with all parameters optimised the average value of α is 0.0512 and CV=37%. Relatively to the undamaged sample, the value of α increased after installation and after ID CE1 the corresponding coefficient of variation increased, while after ID CE2 it decreased (for both the models for b fixed and for b varying during the curve fitting exercise).

Table 3 summarises the values of the tangent stiffness for 2% strain ($J_{t\,2\%}$) obtained from the models (Equation 2, polynomial models; Equation 6 and Equation 8, hyperbolic-based models type A and B, respectively, with all parameters optimised). Additionally, the corresponding secant stiffness ($J_{s\,2\%}$), obtained using Equation 9 is included, to enable direct comparisons to the experimental data.

For both geogrids, the tangent stiffness values obtained from the polynomial and the hyperbolic-based models are different. The values reported for the polynomial models are likely to be more realistic, as these models reproduce very well the experimental responses observed (as illustrated in Figure 4). The secant stiffness values estimated from both polynomial and hyperbolic-based models approximate well the experimental data. The variation of the secant stiffness obtained from the polynomial models relatively to the experimental data ranged between -0.41% and +0.9%. The hyperbolic models led to underesti-

mations of the secant stiffness relatively to experimental data (variations relatively to the experimental results between -5.1% and -21.9%).

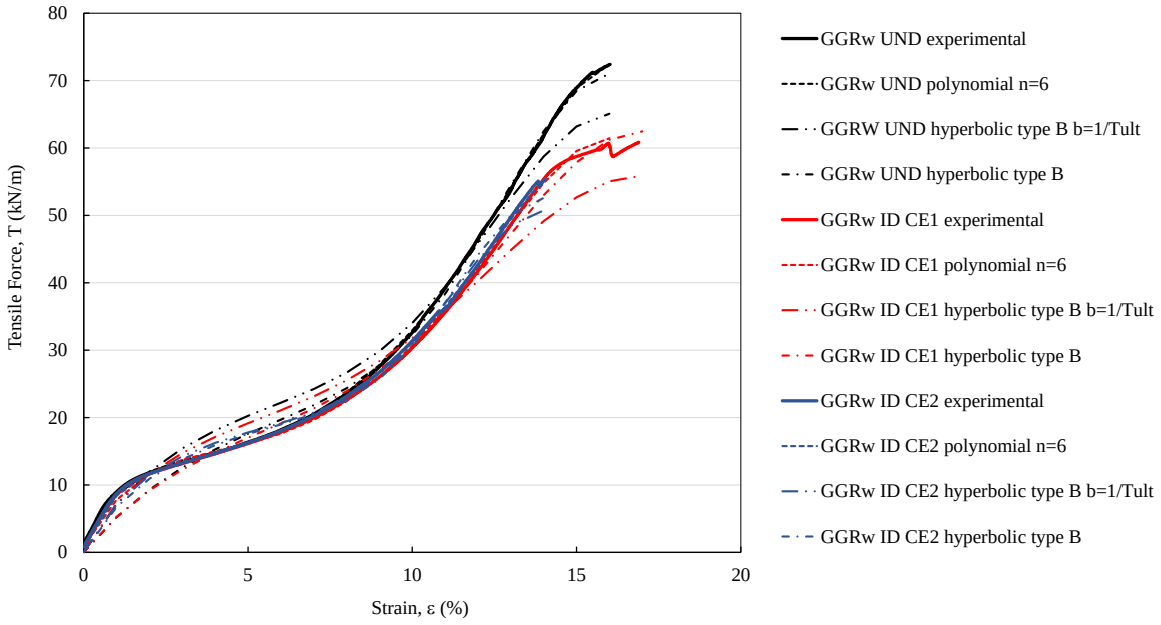

a)

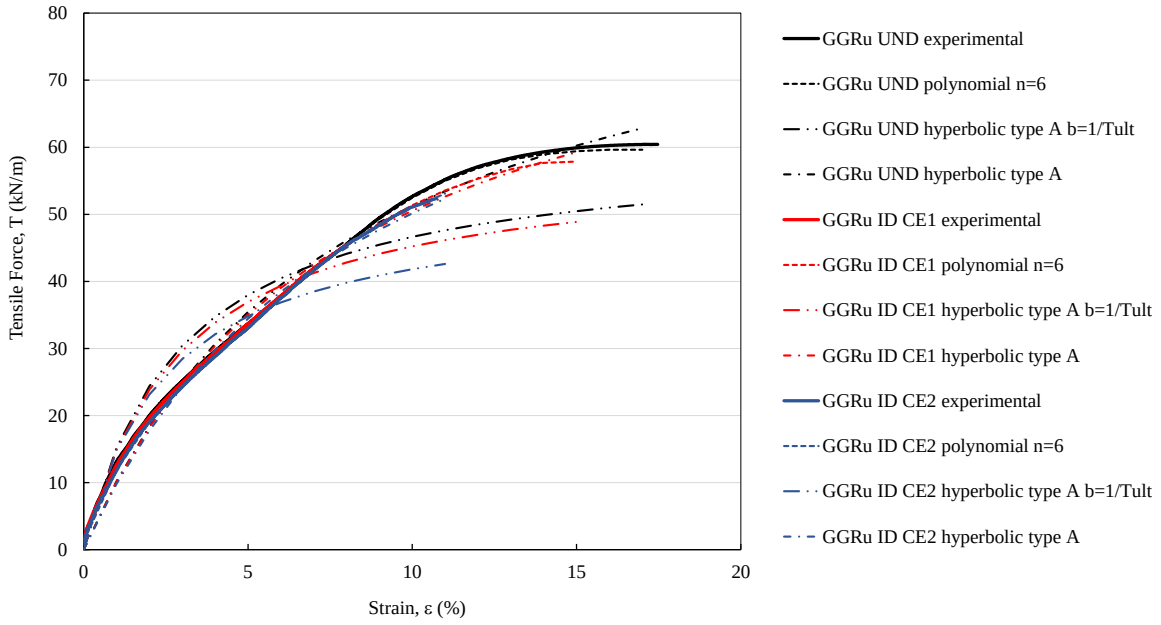

b)

Figure 4. Simple constitutive models (polynomial and hyperbolic-based) representing the tensile response of the geosynthetics studied: a) GGRw (UND specimen 3, ID CE1 specimen 3, ID CE2 specimen 4); b) GGRu (UND specimen 4, ID CE1 specimen 2, ID CE2 specimen 2).

Table 3. Tangent stiffness ($J_{t\ 2\%}$) and secant stiffness ($J_{s\ 2\%}$) for 2% strain obtained from the simple constitutive models for GGRw and GGRu for different types of samples: undamaged (UND) and exhumed after installation damage with compaction energy CE1 and CE2 (ID CE1 and ID CE2, respectively)

Model	Stiffness modulus (kN/m)	GGRw			GGRu		
		UND	ID CE1	ID CE2	UND	ID CE1	ID CE2
Polynomial (n=6)	$J_{t\ 2\%}$	237.3	231.6	225.1	638.4	614.4	617.4
	$J_{s\ 2\%}$	588.1	594.1	585.7	1025.3	976.3	931.0
Hyperbolic-based	$J_{t\ 2\%}$	354.7	345.4	351.2	758.7	727.5	692.8
	$J_{s\ 2\%}$	456.1	512.0	508.1	951.8	908.3	884.3

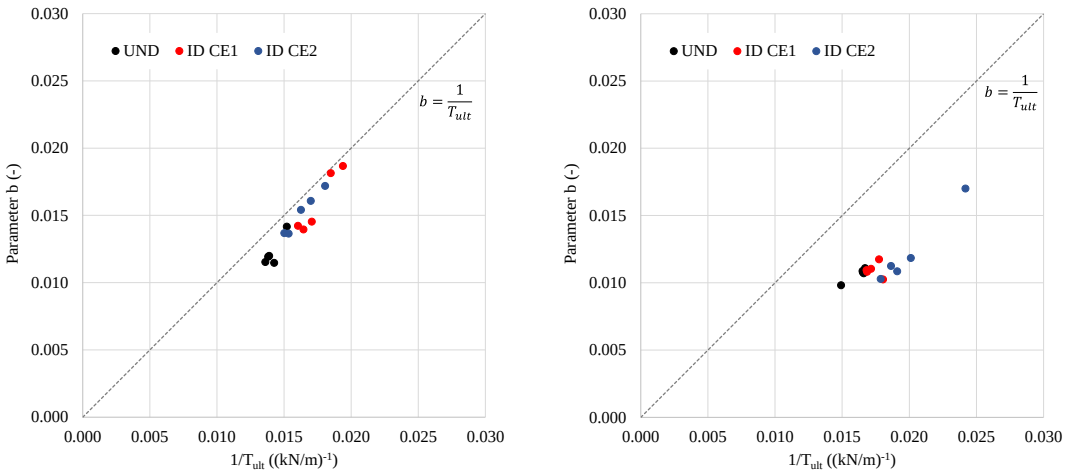

a) b)

Figure 5. Parameter b for the hyperbolic-based models (with all parameters optimised during curve fitting) versus $1/T_{ult}$ for the three types of samples tested (UND, ID CE1, ID CE2): a) GGRw; b) GGRu.

4.3 *Influence of installation damage*

To assess the influence of installation damage on the simple constitutive models used herein to represent the load-strain response of the geogrids studied, the model parameters were analysed and normalised to the reduction factor for installation damage (Figure 6). This reduction factor was taken as the ratio (RF_{ID}, Equation 10) of the tensile strength of the undamaged sample ($\bar{T}_{ult,UND}$) to that of the damaged sample ($\bar{T}_{ult,DAM}$).

$$RF_{ID} = \frac{\bar{T}_{ult,UND}}{\bar{T}_{ult,DAM}} \tag{10}$$

For GGRw and GGRu, there is no clear trend on the influence of installation damage on the polynomial model parameters. For both geogrids, the normalised values of parameter b for the hyperbolic-based models is practically constant, indicating that for these geosynthetics and the installation conditions considered herein, the value of b after installation damage can be obtained from the undamaged sample value divided by the corresponding RF_{ID}. There is no apparent relationship between the model parameters a and α (the latter only applicable to for GGRw) and RF_{ID}.

Figure 6 also includes values of the tangent and secant stiffness for 2% strain normalised to the reduction factor for installation damage. The data indicates that the normalised stiffness is not constant and reduces after installation damage. The retained normalised values (relatively to the undamaged sample) are ~83% for GGRw ID CE1, ~88% for GGR ID CE2, ~90% for GGRu ID CE1 and ~76% for ID CE2.

5 CONCLUSIONS

In this paper, the short-term tensile response of two geogrids was approximated using simple constitutive models. The geosynthetics were exhumed after installation damage under real conditions (one soil and two compaction energies) and the changes in simple constitutive models (polynomial and hyperbolic-based) and the corresponding parameters were analysed. The main conclusions can be summarised as:

- The polynomial models (order 6) approximated the short-term tensile experimental data better than the hyperbolic-based models.
- Contrary to what has been reported in the literature, for the materials and test conditions presented herein, the parameter b of the hyperbolic-based models could not be estimated as the inverse of the materials tensile strength.
- Additionally, for GGRw the parameter α of the hyperbolic-based models was not constant (again, contrary to what has been reported in the literature) with a coefficient of variation of 40% for the undamaged sample.
- Both polynomial and hyperbolic-based models approximated well the secant stiffness for 2% obtained experimentally; the polynomial model estimates were very close to the experimental data, while the values obtained from the hyperbolic-based model underestimated the secant stiffness for 2% strain.

- The model parameters were normalised to the reduction factor for installation damage. For the polynomial models, no clear trend was found. For the hyperbolic-based models, the parameter b was practically unchanged after exhumation of the samples, while parameters a and α showed no clear trend.
- The values of the stiffness normalised to the reduction factor for installation damage were not constant, but they all exhibited retained values ranging between 76% and 90% relatively to the undamaged samples.

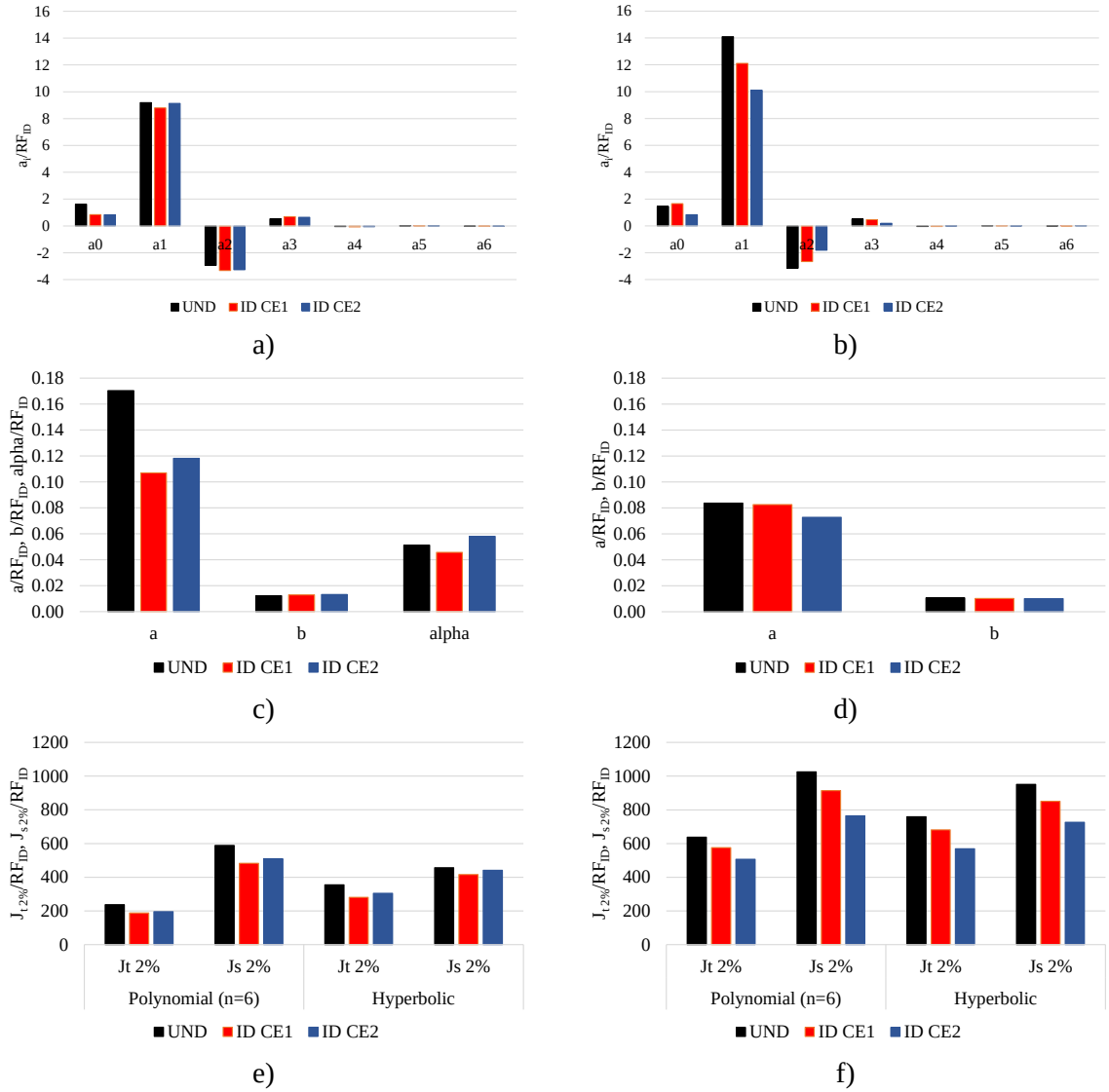

Figure 6. Model parameters and stiffness normalised relatively to the reduction factor for installation damage (RF_{ID}) for the three types of samples tested (UND, ID CE1, ID CE2): a_i/RF_{ID} for the polynomial models and a/RF_{ID}, b/RF_{ID} and α/RF_{ID} for the hyperbolic-based models (with all parameters optimised during curve-fitting), tangent and secant stiffness for 2% strain (a), c) and e) GGRw, b), d) and f) GGRu).

REFERENCES

Allen, T.M. & Bathurst, R.J. 1994. Characterization of geosynthetic load-strain behavior after installation damage. Geosynthetics International, 1(2), pp. 181–199.

Bathurst, R.J. & Kaliakin, V.N. 2005. Review of numerical models for geosynthetics in reinforcement applications. Computer Methods and Advances in Geomechanics: 11th International Conference of the International Association for Computer Methods and Advances in Geomechanics, 19-24 June 2005, Torino, Italy, Vol. 4, 407-416.

BSI 2008. EN ISO 10319. Geosynthetics. Wide-width tensile test. BSI, London, UK.

Liu, H. & Ling, H.I. 2007. Unified Elastoplastic-Viscoplastic Bounding Surface Model of Geosynthetics and Its Applications to Geosynthetic Reinforced Soil-Retaining Wall Analysis. Journal of Engineering Mechanics 133(7), pp. 801-815.

Pinho-Lopes, M. & Lopes, M.L. 2014. Tensile properties of geosynthetics after installation damage. Environmental Geotechnics 1(3), pp. 161-178.